Supplementary information

Backbone engineering of *N,N,N′,N′*-tetraphenyl-1,4-phenylenediamine-based conjugated porous polymers toward enhanced electrochromic behavior

Mengfan Zhang, Xiujuan Zhong, Shouli Ming, Yan Zhang* and Jinsheng Zhao*

Shandong Key Laboratory of Chemical Energy Storage and New Battery Technology, School of Chemistry and Chemical Engineering, Liaocheng University, Liaocheng, 252000, P. R. China.
E-mail: zy@lcu.edu.cn (Y. Zhang), j.s.zhao@163.com (J.S. Zhao)

Materials

(E)-1,2-Bis(5-(trimethylstannyl)thiophen-2-yl)ethene (TVT-2Sn, 98%) and (E)-2,3-bis(5-(trimethylstannyl)thiophen-2-yl)acrylonitrile (TVTCN-2Sn, 98%) were purchased from Derthon Optoelectronic Materials Science Technology Co., Ltd. (Shenzhen, China). *N1,N1,N4,N4*-tetrakis(4-bromophenyl)benzene-1,4-diamine (TPPA-4Br, >95%) was purchased from Jilin Chinese Academy of Sciences-Yanshen Technology Co., Ltd. (Changchun, China). Bis(triphenylphosphine)palladium(II) chloride ($Pd(PPh_3)_2Cl_2$, 98%) was purchased from Hebei Bailingwei Super Fine Material Co., Ltd. (Langfang, China). Tetrabutylammonium hexafluorophosphate ($TBAPF_6$, 98%) was purchased from Shanghai Macklin Biochemical Co., Ltd. (Shanghai, China). Acetonitrile (ACN) was purchased from Aladdin Chemical Co., Ltd. (Shanghai, China). Toluene, methanol, chloroform, and anhydrous ethanol were purchased from Yantai Yuandong Fine Chemical Co., Ltd. (Yantai, China). Indium-tin-oxide (ITO) coated glass (sheet resistance: < 10 Ω/sq) was purchased from Zhuhai Kaivo Optoelectronic Technology Co., Ltd. (Zhuhai, China).

Instrument and Characterization

X-ray diffraction (XRD) patterns were acquired on a Kigaka D/max 2500 Cu-Kα radiation X-ray advance diffractometer in the 2θ range of 3º to 80º. Fourier transform infrared (FTIR) spectroscopy was performed using a Nicolet Avatar 360 FT-IR

spectrometer. Solid state ^{13}C CP/MAS NMR spectroscopy was performed using a Bruker Avance Neo 400WB solid state NMR spectroscopy. X-ray photoelectron spectroscopy (XPS) was carried out using a Thermo ESCALAB 250Xi spectrometer. The surface morphology was obtained by a Thermo Fisher Scientific FIB-SEM GX4 scanning electron microscope (SEM). The specific surface area and pore size distribution were determined from the N_2 adsorption-desorption isotherm measured at 77.3 K using an ASAP 2460-3 (Micromeritics) volumetric adsorption analyzer.

Density functional theory (DFT) calculations were carried out using the Gaussian 16 program with the B3LYP/6-31G (d,p) basis set [S1] to determine the optimized geometries, frontier molecular orbitals (FMOs), and surface electrostatic potential (ESP) maps of the repeating units.

The electrochemical behavior of the polymer films was studied using cyclic voltammetry (CV) on a CHI 760C electrochemical workstation. All CV experiments were performed in an ACN solution with 0.1 M $TBAPF_6$ as the supporting electrolyte under argon protection. A platinum wire was employed as the counter electrode, a silver wire as the reference electrode, and ITO glass coated with the polymer film as the working electrode. The scan rate was set at 100 mV/s.

Optical absorption measurements were performed using a HITACHI UH4150 spectrophotometer. Spectroelectrochemical and kinetic switching experiments were also conducted on the HITACHI UH4150 spectrophotometer, and the required applied voltages were provided by the CHI 760C electrochemical workstation. In the kinetic switching experiments, the test wavelengths were the maximum absorption wavelengths (λ_{max}) of the polymers, except that 510 nm was selected for P(TPPA-TVTCN) in the visible region due to the higher optical contrast at this wavelength compared to that at its λ_{max} (495 nm). The polymer film covered an area of 0.9 cm × 3.0 cm on the ITO electrode.

Colorimetric tests were carried out using an X-Rite Ci7600 spectrophotometer. The color variations of the polymers were depicted using the CIE 1976 $L^*a^*b^*$ color space. In this system, L^* represents lightness, a^* represents the color variation from green to red, and b^* represents the color variation from blue to yellow.

Coloration efficiency (CE) is defined as the change in optical density (ΔOD) per unit charge density (ΔQ). The calculation formula is:

$$CE = \frac{\Delta OD}{\Delta Q} = \frac{lg(T_b/T_c)}{Q/A}$$

Here, T_b and T_c represent the transmittance of the polymer film at the specific wavelengths in the bleached and colored states, respectively. Q is the amount of injected charge, and A is the effective area of the film on the ITO electrode.

Synthesis of P(TPPA-TVT)

P(TPPA-TVT) was prepared via the Stille coupling reaction. TPPA-4Br (43.69 mg, 0.06 mmol) and TVT-2Sn (62.15 mg, 0.12 mmol) were added to a Schlenk flask along with 30 mL of toluene. The mixture was sonicated for 10 minutes to ensure complete dissolution. Under a nitrogen atmosphere, the catalyst $Pd(PPh_3)_2Cl_2$ (4.21 mg, 0.006 mmol) was added to the reaction mixture. Subsequently, the ITO glass, which had been ultrasonically cleaned with deionized water and ethanol, was vertically positioned inside the Schlenk flask. After three cycles of vacuum evacuation and nitrogen purging, the flask was sealed under a nitrogen atmosphere and the internal mixture was subjected to reaction at 110 °C for 72 hours. During the reaction process, a thin polymer film was formed on the surface of the ITO glass through the liquid/solid interfacial solvothermal method. After the reaction was completed, the ITO glass coated with the polymer was rinsed several times with anhydrous methanol and then with chloroform, and the resulting film appeared orange-yellow. The precipitate in the Schlenk flask was collected by filtration, washed with anhydrous methanol three times, and finally purified using the Soxhlet extraction method. The solvents for Soxhlet extraction were chloroform and anhydrous ethanol, with each solvent used sequentially for 24 hours. After vacuum drying, the P(TPPA-TVT) powder was obtained, and it appeared orange-red.

Synthesis of P(TPPA-TVTCN)

The synthesis and purification steps of P(TPPA-TVTCN) were consistent with those of P(TPPA-TVT). The reagents used are listed below: TPPA-4Br (29.12 mg, 0.04 mmol), TVTCN-2Sn (43.43 mg, 0.08 mmol), toluene (30 mL) and $Pd(PPh_3)_2Cl_2$ (2.81 mg, 0.004 mmol). The resulting polymer film appeared brick-red, while the corresponding powder was blackish-red.

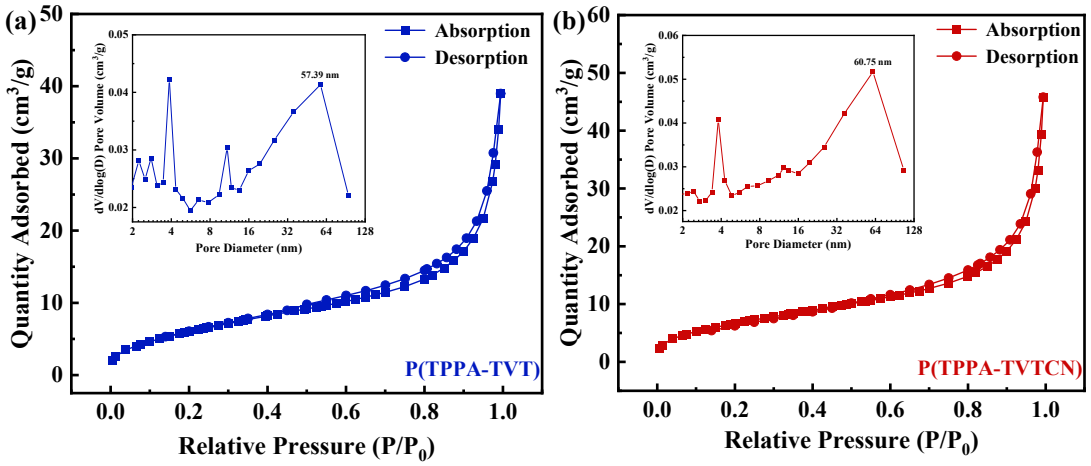

Fig. S1. N_2 adsorption-desorption isotherms and pore size distributions of (a) P(TPPA-TVT) and (b) P(TPPA-TVTCN).

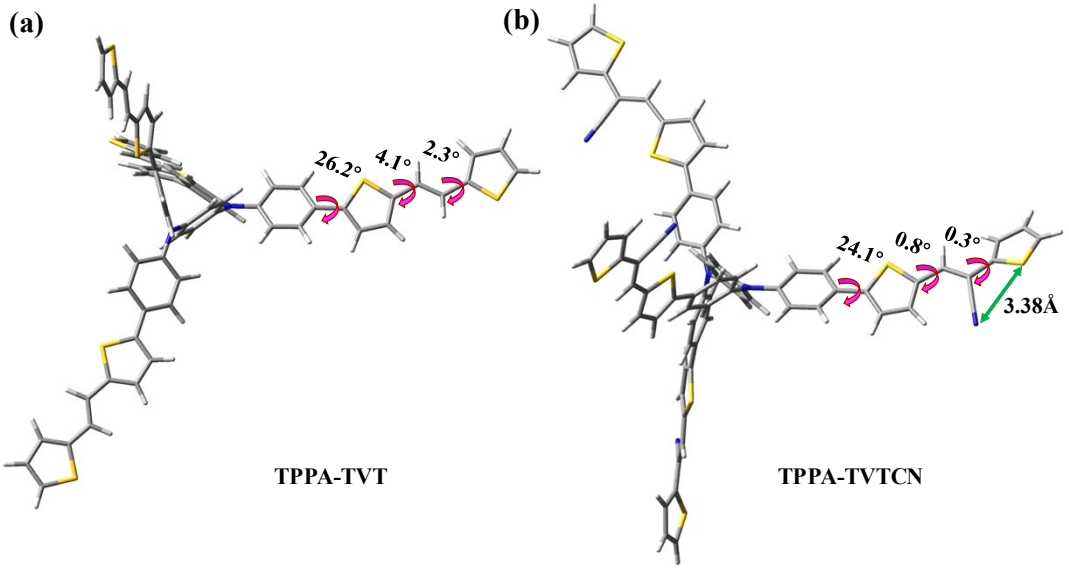

Fig. S2. Optimized geometries of (a) TPPA-TVT and (b) TPPA-TVTCN. The grey, white, yellow and blue atoms denote the C, H, S and N atoms, respectively.

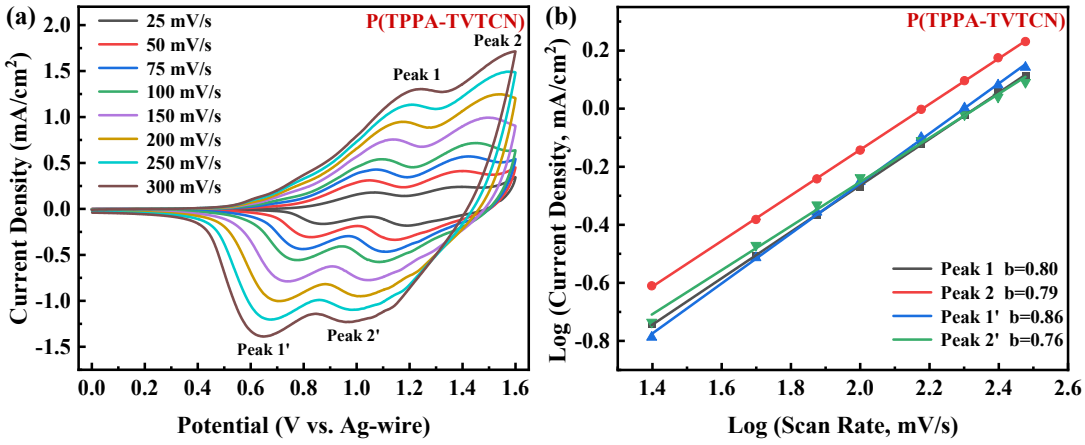

Fig. S3. (a) CV curves at various scan rates and (b) log(*j*) versus log(*v*) plots of P(TPPA-TVTCN).

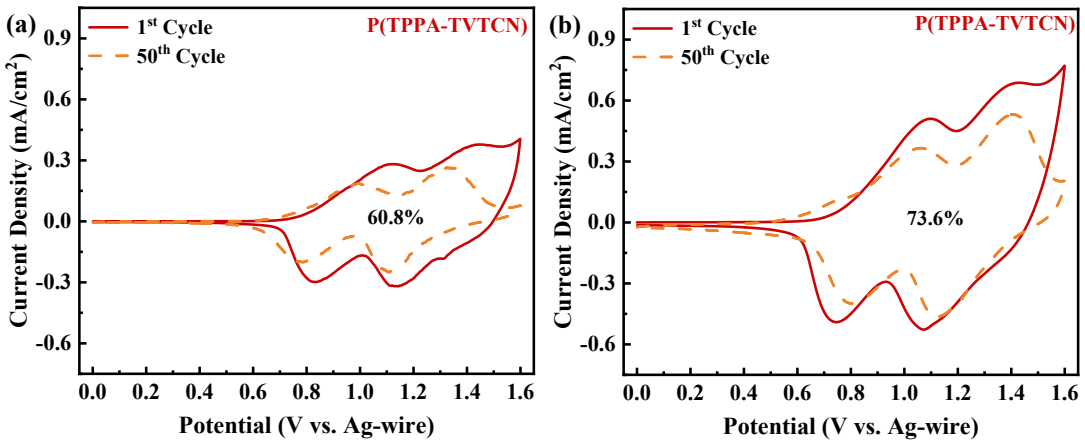

Fig. S4. The first and the 50th CV curves of P(TPPA-TVTCN) at (a) 50 mV/s and (b) 100 mV/s.

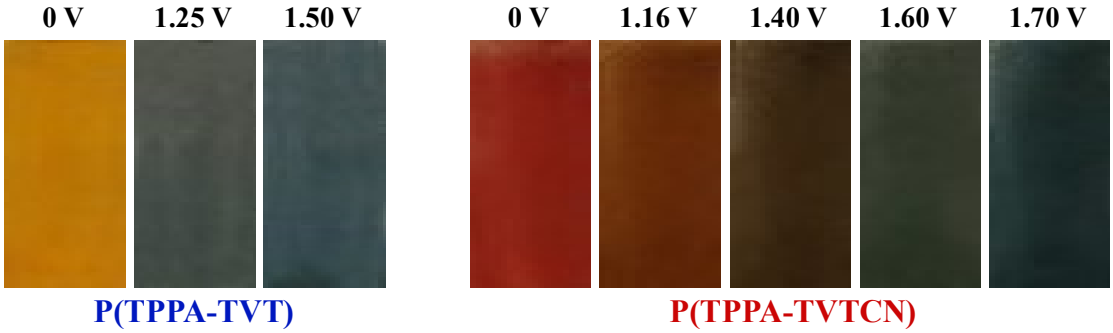

Fig. S5. Color evolution of (a) P(TPPA-TVT) and (b) P(TPPA-TVTCN) during stepwise oxidation.

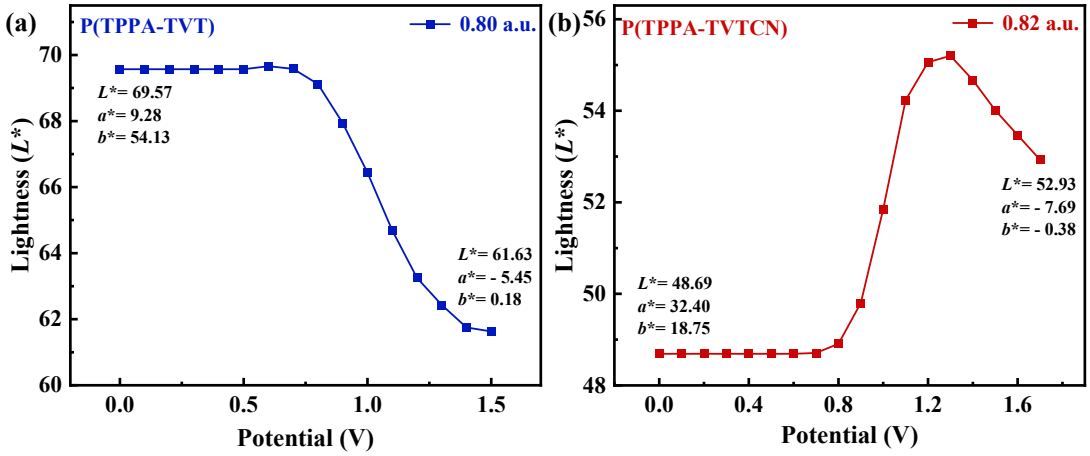

Fig. S6. Colorimetric L^* values of (a) P(TPPA-TVT) and (b) P(TPPA-TVTCN) as a function of applied potential.

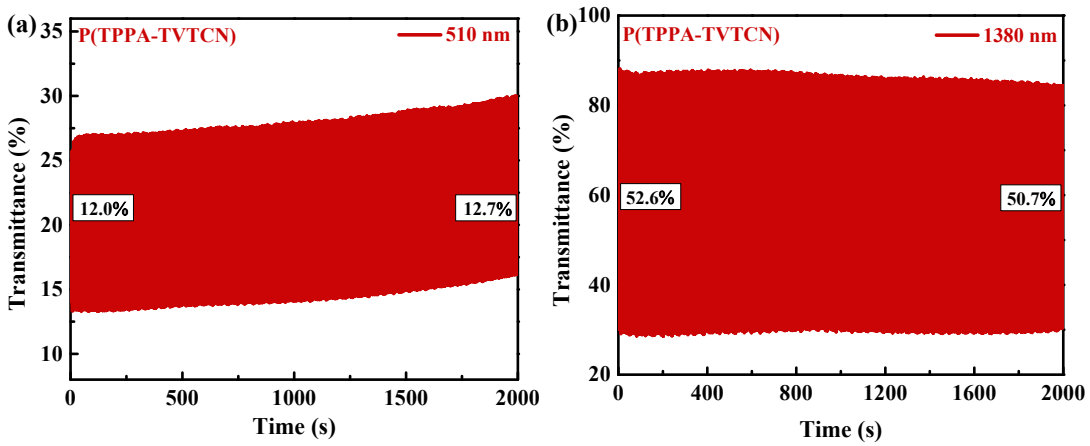

Fig. S7. Transmittance switching of P(TPPA-TVTCN) (a) at 510 nm and (b) at 1380 nm for 2000 seconds testing time.

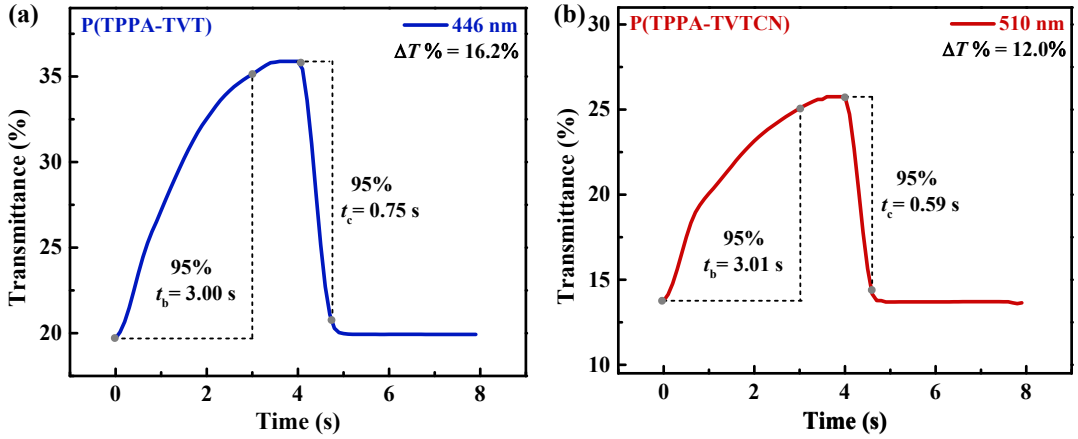

Fig. S8. Response times of (a) P(TPPA-TVT) at 446 nm and (b) P(TPPA-TVTCN) at 510 nm.

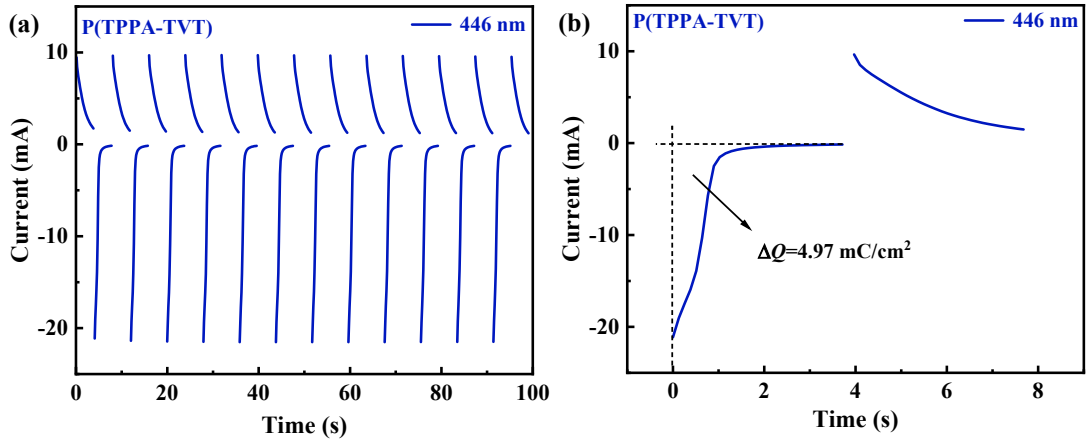

Fig. S9. (a) Current-time curve and (b) charge consumption per unit area during the dedoping process of P(TPPA-TVT) at 446 nm.

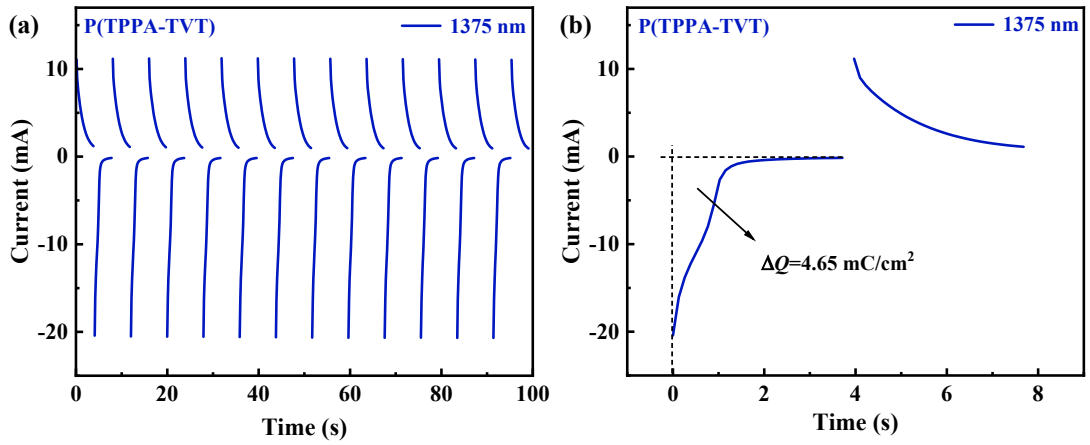

Fig. S10. (a) Current-time curve and (b) charge consumption per unit area during the dedoping process of P(TPPA-TVT) at 1375 nm.

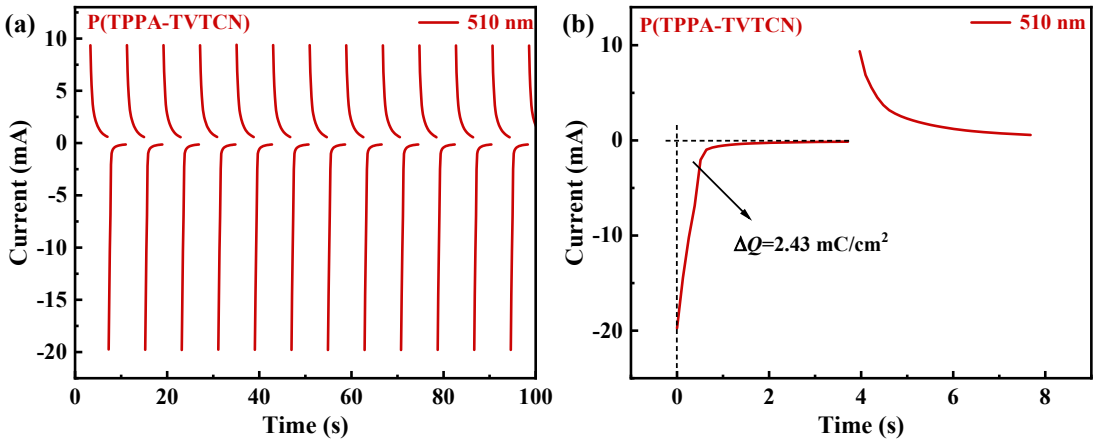

Fig. S11. (a) Current-time curve and (b) charge consumption per unit area during the dedoping process of P(TPPA-TVTCN) at 510 nm.

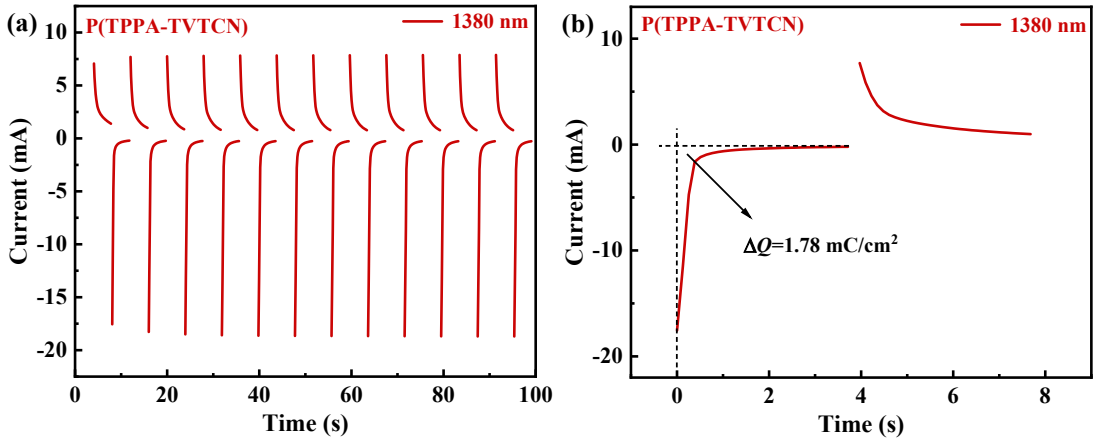

Fig. S12. (a) Current-time curve and (b) charge consumption per unit area during the dedoping process of P(TPPA-TVTCN) at 1380 nm.

Table S1 Color change, kinetic parameters, and cycling stability of P(TPPA-TVT), P(TPPA-TVTCN), and several reported TPPA-based electrochromic polymers.

Polymer	Unit structure	Color change	λ (nm)	ΔT% (%)	$t_{95\%}$ (s)		CE (cm²/C)	Cycling stability
					t_b	t_c		
P(TPPA-TVT) (this work)	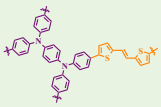		446	16.2	3.00	0.75	52.42	79.0% (1000 s)
			1375	49.1	0.91	2.10	93.46	84.5% (1000 s)
P(TPPA-TVTCN) (this work)	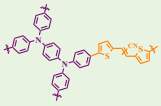		510	12.0	3.01	0.59	112.07	No ΔT% drop (2000 s)
			1380	52.6	0.76	2.05	231.52	96.4% (2000 s)
P(TPPA-BTP) [S2]	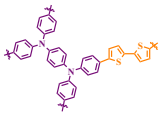		430	28.7	3.07	0.88	256.20	89.2% (1500 s)
			1380	57.0	1.77	1.59	170.20	61.1% (1500 s)
P-TBDA [S3]	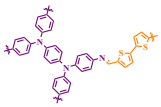		776	36.0	1.80	2.50	-	80.0% (1500 s)
			947	37.5	2.00	2.40	-	80.0% (1000 s)
TPPA-BTT-CPP [S4]	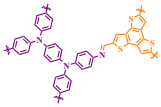		1080	47.1	1.06	1.76	234.80	88.3% (2000 s)
$COF_{TPDA-PDA}$ [S5]	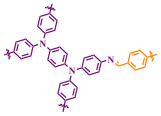		1050	52.0	0.70	1.30	320.00	No ΔT% drop (20 cycles)
TAPD-TDA COF [S6]	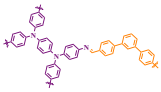		1060	34.3	5.10	25.8	249.90	No ΔT% drop (20 cycles)
EC-COF-1 [S7]	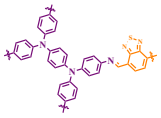		574	33.0[a]	7.2[a]	1.8[a]	284.00[a]	99.7%[a] (900 s)
			730	12.0[a]	3.5[a]	2.6[a]	246.00[a]	99.5%[a] (900 s)

[a] The data correspond to the respective devices.

References

S1 M. J. Frisch, G. W. Trucks, H. B. Schlegel, G. E. Scuseria, M. A. Robb, J. R. Cheeseman, G. Scalmani, V. Barone, G. A. Petersson, H. Nakatsuji, X. Li, M. Caricato, A. V. Marenich, J. Bloino, B. G. Janesko, R. Gomperts, B. Mennucci, H. P. Hratchian, J. V. Ortiz, A. F. Izmaylov, J. L. Sonnenberg, D. Williams-Young, F. Ding, F. Lipparini, F. Egidi, J. Goings, B. Peng, A. Petrone, T. Henderson, D. Ranasinghe, V. G. Zakrzewski, J. Gao, N. Rega, G. Zheng, W. Liang, M. Hada, M. Ehara, K. Toyota, R. Fukuda, J. Hasegawa, M. Ishida, T. Nakajima, Y. Honda, O. Kitao, H. Nakai, T. Vreven, K. Throssell, J. A. Montgomery, Jr., J. E. Peralta, F. Ogliaro, M. J. Bearpark, J. J. Heyd, E. N. Brothers, K. N. Kudin, V. N. Staroverov, T. A. Keith, R. Kobayashi,

J. Normand, K. Raghavachari, A. P. Rendell, J. C. Burant, S. S. Iyengar, J. Tomasi, M. Cossi, J. M. Millam, M. Klene, C. Adamo, R. Cammi, J. W. Ochterski, R. L. Martin, K. Morokuma, O. Farkas, J. B. Foresman and D. J. Fox, Gaussian, Inc., Wallingford CT, Gaussian 16, Revision C.01, 2016.

S2 X. Bo, X. Zhong, S. Ming, Y. Zhang and J. Zhao, *Eur. Polym. J.*, 2025, **230**, 113894.

S3 K. Feng, X. Wang, H. Zhang, H. Shen, X. Shi, Z. Xing, B. Wang, Z. Li, Z. Chen and Z. Jiang, *Chem. Eng. J.*, 2025, **524**, 169141.

S4 X. Liu, F. Zhao, S. Ming, Y. Zhang and J. Zhao, *Eur. Polym. J.*, 2024, **208**, 112853.

S5 Q. Hao, Z. J. Li, B. Bai, X. Zhang, Y. W. Zhong, L. J. Wan and D. Wang, *Angew. Chem. Int. Ed.*, 2021, **60**, 2–8.

S6 P. Shi, J. Wang and Z. Guo, *Chem. Eng. J.*, 2023, **451**, 139082.

S7 F. Yu, W. Liu, S. W. Ke, M. Kurmoo, J. L. Zuo and Q. Zhang, *Nat. Commun.*, 2020, **11**, 5534.